# Convergent Functional Groups. 3. A Molecular Cleft Recognizes Substrates of Complementary Size, Shape, and Functionality

**J. Rebek, Jr.,* B. Askew, M. Killoran, D. Nemeth, and F.-T. Lin**

Contribution from the Department of Chemistry, University of Pittsburgh, Pittsburgh, Pennsylvania 15260. Received July 21, 1986

Abstract: Model systems for molecular recognition are reviewed, and attention is drawn to special problems encountered with *macrocyclic* receptors. A series of rigid structures is examined in which two carboxylic acids converge to define a *molecular cleft*. Through NMR methods it is possible to show that small molecules of complementary size, shape, and functionality bind within the cleft. Heterocyclic diamines are especially suitable substrates because their binding involves ionic as well as hydrogen-bonding interactions with the receptors. Pyrazine, pyrimidine, purine, and other imidazole derivatives are shown to interact with the receptors to give complexes of well-defined geometry. Optimal binding occurs to those substrates which are *chelated* by the receptors and provide complementary surfaces for aryl–aryl stacking interactions. The origins of selectivity for other model receptors are outlined, and the advantages of convergent functional groups, capable of bonding interactions of a directional sort, are described.

Molecular recognition is widespread. It lies at the heart of enzyme and receptor specificity, it is the source of reagent selectivity in organic synthesis, and it is a current, fashionable pursuit of bioorganic chemistry. In this last context practitioners are concerned with complexing small molecules by larger ones with the ultimate intent of performing chemical operations on the complex. The first step involves the matching of shapes between receptor and substrate, and the most readily available receptors have had macrocyclic shapes: cyclodextrins, crown ethers, and cyclophanes. The complexation has thereby been simplified to the conceptually appealing and satisfying filling of holes (eq 1).

$$\bigcirc + \bullet \rightleftharpoons \circledcirc \quad (1)$$

**Macrocyclic receptor**   **Substrate**   **Complex**
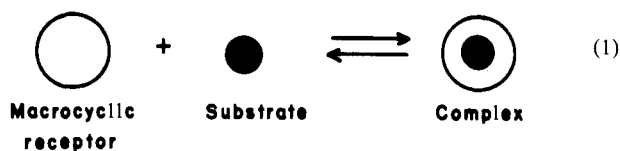
The reaction step in the sequence poses a more difficult problem. Functional groups on the receptor must find their complements on the substrates, so the selection of reaction type is determined by which functional groups on substrate and receptor are likely to be properly arranged for reaction in the complex. Macrocyclic structures, however, are difficult to functionalize with reactive groups that *converge* on the guest molecule. The topology of such

Divergent Functional Groups (F) on Cyclodextrins and Crown Ethers
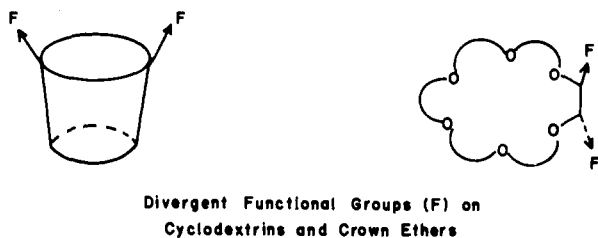
systems favors reagent approach to the outer surface and leads to auxiliary functionality which diverges; functional groups become directed away from the bound substrates in a molecular version of the "maginot line". For example, cyclodextrins are readily derivatized on their rims but not on their interior surfaces, and considerable molecular scaffolding is required to bring catalytically useful groups to bear on the substrates held inside.[1a–c] Similar

problems are encountered in crown ether chemistry.[1d–f]

In a new approach to these issues we introduced[2a] the structures **1** and **2** and presented evidence of their unusual behavior.[2b–d] These structures incorporate carboxyl groups which *converge on*

1   **2**
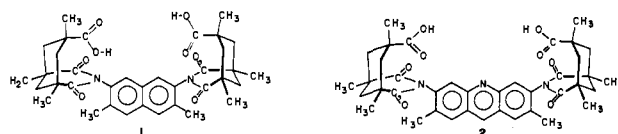
a molecular cleft, in a manner that resembles the convergence of functional groups at the active sites of enzymes. Our premise was that the functional groups which line the cleft can bind substrates and are also poised to practice chemistry on them. In the sequel, we shall explore the catalytic advantages that accrue when such structural features are present. Here, we examine their more static properties as receptors for molecules of complementary size, shape, and functionality.

Synthesis

The receptors are rapidly and efficiently assembled from the appropriate aromatic diamines by merely heating them with the triacid **3** in the absence of solvent. The syntheses of the fluorene derivative **4** and acridine derivative **5** from their respective aromatics are exemplary.


4   **5**
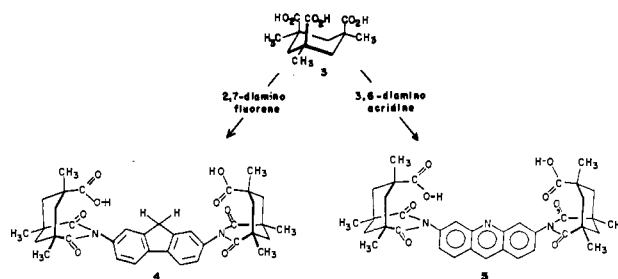
The triacid **3** was first prepared by Kemp[3] through an oxidative degradation of trimethyl adamantanol, but because the latter is no longer available in quantity from commercial sources, an alternate synthesis was developed. The new method involves the straightforward trimethylation of **6** with Me_2SO_4 mediated by

(1) (a) Breslow, R.; Hammond, M.; Lauer, M. *J. Am. Chem. Soc.* **1980**, *102*, 421–422. (b) Tabushi, I. *Acc. Chem. Res.* **1982**, *15*, 66–72. (c) Winkler, J.; Coutouli-Argyropoulou, E.; Leppkes, R.; Breslow, R. *J. Am. Chem. Soc.* **1983**, *105*, 7198–7199. (d) Chao, Y.; Weisman, G. R.; Sogah, G. D. Y.; Cram, D. J. *J. Am. Chem. Soc.* **1979**, *101*, 4948–4958. (e) Lehn, J.-M. *Science (Washington, DC)* **1985**, *227*, 849–856. (f) Sasaki, S.; Shionoya, M.; Koga, K. *J. Am. Chem. Soc.* **1985**, *107*, 3371–3372.

(2) (a) Rebek, J., Jr.; Marshall, L.; Wolak, R.; Parris, K.; Killoran, M.; Askew, B.; Nemeth, D.; Islam, N. *J. Am. Chem. Soc.* **1985**, *107*, 7476–7481. (b) Rebek, J., Jr.; Marshall, L.; McMannis, J.; Wolak, R. *J. Org. Chem.* **1986**, *51*, 1649–1653. (c) Rebek, J., Jr.; Nemeth, D. *J. Am. Chem. Soc.* **1985**, *107*, 6738–39. Rebek, J., Jr.; Askew, B.; Islam, N.; Killoran, M.; Nemeth, D.; Wolak, R. *J. Am. Chem. Soc.* **1985**, *107*, 6736–38.

(3) Kemp, D. S.; Petrakis, K. S. *J. Org. Chem.* **1981**, *46*, 5140–5143.

lithium diisopropylamide[4] (LDA) (eq 2). The triester **6** is readily obtained from trimesic acid through hydrogenation[5a] then esterification (SOCl$_2$/MeOH).

(2)
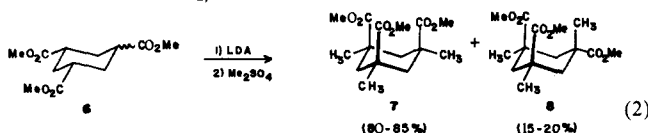
The alkylation can be controlled to give a preponderance of the desired isomer **7**, which is separated from the cis, trans isomer **8** by either fractional crystallization or preparative HPLC. Saponification of **7** then gives **3**. The synthesis has been carried out on a 100-g scale without inconvenience and delivers a 50–60% yield from **6**.

Structure

Despite the rigidity imparted by the aromatic and cyclohexane subunits, there are two dynamic features in the new structures. The first involves proton-transfer reactions and these are particularly apparent in those molecules which incorporate acridine nuclei as spacer groups. In the absence of added acids or bases, **2** and **5** show exchange-broadened NMR signals at room temperature (300 MHz) for the aromatic hydrogens in nonpolar solvents such as CDCl$_3$. This broadness was constant in the concentration range 2×10^{-3}–9×10^{-4} M. This behavior can be attributed to eq 3, the rates of which occur in the intermediate

(3)
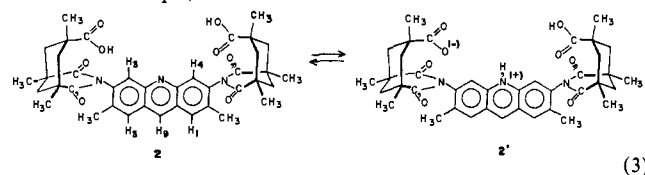
NMR time frame in CDCl$_3$. At low temperature (200 K) a complicated spectrum is observed in the aromatic region. The reason for the relative slowness of this proton transfer is not clear. Both **2** and **5** contain 2–3 molecules of water from which they are very difficult to separate, and these "packed" water molecules are expected to provide a reasonable bridge for the proton transfer of eq 3. Indeed, in wet CD$_2$Cl$_2$ the relatively sharp spectrum is temperature independent. In CD$_3$OD, the signals sharpen and the zwitterionic form predominates, i.e., the NMR signal for H$_9$ (9.2 ppm) in this solvent appears at the same shift as it does in the picrate of **2** in CDCl$_3$. Addition of other strong acids, e.g., toluenesulfonic acid, also sharpened the aromatic signals and gave the same shift for H$_9$.

Addition of bases such as Et$_3$N also sharpened the NMR signals of **2** in CDCl$_3$. In this case H$_4$ and H$_5$ the "interior protons" shift downfield to 8.45 ppm and H$_9$ appears at 8.7 ppm. That proton-transfer reactions caused the broadened spectra of **2** was firmly established by the conversion of **2** to its dimethyl ester **2a** and amide **2b** (eq 4). Both of these showed sharp spectra, and in

(4)
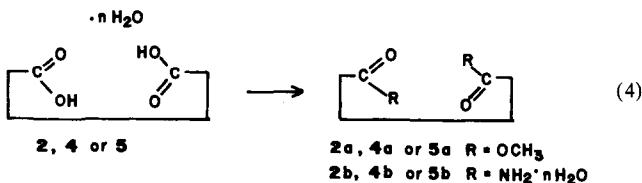
accord with Wolfenden's[6] findings on the affinity of various functional groups for water, the amide **2b** but not the ester **2a** was heavily "waterlogged".

The second dynamic aspect of the new molecules involves the rotation about the C$_{aryl}$–N$_{imide}$ bonds in those structures such as **5** and the fluorene derivative **4** which have no substituents *ortho*

to the amine. In agreement with our earlier findings,[2a] activation barriers for this rotation are ~13 kcal/mol; this barrier height and the differences in frequency involved usually result in coalescence below room temperature. The ambient temperature 300-MHz NMR spectra are therefore on the rapid but still somewhat broadened end of the scale.

Because of the proton-transfer reactions described above, the isolated dynamics of the *rotations* were examined with the dimethyl esters of both the acridine **5a** and fluorene **4a**. At low temperatures (195 K) the slow exchange limit was reached for **5a** but considerable overlap of the spectra of the three conformational isomers occurs (these arise from the perpendicular arrangement of imide and aromatic functions[2a]), and assignments could not be made with certainty. Similar situations held in the case of the fluorene diester **4a**, but the benzyl protons and methyl ester signals were resolved at low temperatures and showed a statistical distribution (1:2:1) of the convergent, in–out, and divergent conformations of the carboxyl functions shown schematically below
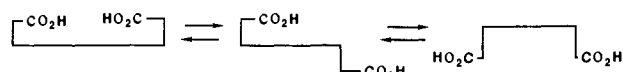
The two dynamic aspects mentioned above do not entirely account for the broadened spectrum of the fluorene diacid **4** in CDCl$_3$. Addition of carboxylic acids (HOAc) to such solutions sharpens the spectrum to that expected for the rapid exchange limit. However, it is unlikely that added acids increase (or decrease) the rotation rates; they must increase the proton-transfer rates, but just which proton-transfer reactions are involved is hard to specify. There is bound water in these molecules and perhaps the broadness is due to various states of ionization involving the bound water and the carboxylic acid functions.

Unlike conventional carboxylic acids, which are extensively in the form of cyclic, hydrogen-bonded dimers in nonpolar solvents,[7] the carboxyl functions of the new acids are sufficiently buried that such dimerization is discouraged by steric effects. Hydrogen-bonded chains appear possible, but such chains are expected to be rapidly formed and dissipated. Perhaps mixed dimers are formed between these acids and added HOAc. At present, we have no satisfactory explanation for the salubrious effect of acids on the spectra of **4**.

Finally, the hydrolytic stability of the new structures varies. The naphthalene **1** and fluorene derivatives **4** are quite stable to aqueous acids and bases, e.g., saponification of esters takes place without damage to the imide functions. Derivatives of the acridines, however, slowly hydrolyze in contact with aqueous solutions. For example, overnight stirring of a solution of **2** in CHCl$_3$ overlayered with H$_2$O led to only 30–50% recovery. Presumably, the protonation of the acridine nitrogen is the source of this sensitivity, since it exposes the imides to the destructive advances of external or even internal nucleophiles. A reasonable, but untested mechanism is suggested in eq 5.

(5)
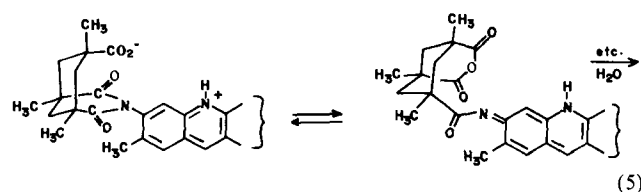
Complexation

1. Diamines. Given the acidic functions of the receptor molecules, it was hardly surprising to find that they would form chelate-type complexes with appropriate diamines. Conventional acid/base chemistry did, in fact, occur when the acridine yellow derivative **2** was as treated with the bases Et$_3$N, morpholine, and diazabicyclooctane (DABCO) in CDCl$_3$. These were charac-

(4) Shiner, V. J., Jr.; Tai, J. J. *J. Am. Chem. Soc.* **1981**, *103*, 436–442.
(5) (a) Steitz, A., Jr. *J. Org. Chem.* **1968**, *33*, 2978–2979. (b) Newman, M. S.; Lowrie, H. S. *J. Am. Chem. Soc.* **1954**, *76*, 4598–4600.
(6) Wolfenden, R. *Science (Washington, DC)* **1983**, *222*, 1087–1093.

(7) Hadzi, D.; Detoni, S. In *The Chemistry of Carboxylic Acid Derivatives*; Patai, S., Ed.; John Wiley & Sons: New York, 1979; Supplement B, Part 1, pp 214–241.

Table I. Association Constants[a] for Complexes of **2**, $CDCl_3$, 25 °C

$$\text{base} + 2 \underset{}{\overset{K_a}{\rightleftharpoons}} \text{complex}$$

| base	K_a (M⁻¹)	pK_a[b] (BH⁺)
DABCO	1.6×10^5	8.2, 4.2
pyrazine **9**	1.4×10^3	0.65
quinoxaline **10**	23×10^3	0.56
phenazine **11**	2.2×10^3	1.2
pyrimidine **16**	0.7×10^3	1.3
quinazoline **17**	1.6×10^3	1.9[c]
imidazole **18**	$K_1 = 1.0 \times 10^6$, $K_2{}^d = 5.5 \times 10^4$	6.9
benzmidazole **20**	$K_1 = 1.5 \times 10^4$, $K_2{}^d = 7.5 \times 10^3$	5.5
purine[e] **21**	$\sim 8 \times 10^3$	2.4
pyridine	$K_1 = 1.2 \times 10^2$, $K_2{}^d = <1$	5.2

[a]Obtained from Eadie–Hofstee[11] or Benesi–Hildebrand[9] plots involving chemical shift changes as a function of receptor/substrate ratios. Saturation of the receptor (>95% sites occupied) was attained with all bases except pyridine. [b]Albert, A. In *Physical Methods in Heterocyclic Chemistry*; Katritzky, A., Ed.; Academic Press: New York, 1963; Vol. I, Chapter 1. [c]For the unhydrated form: *The Chemistry of Heterocyclic Compounds*; Brown, D. J., Ed.; Interscience: New York, 1967; Vol. 24, Part 2 (Quinazolines), Chapter II. [d]($M^{-2} \, 1^2$). [e]Low solubility of this base required such high dilution that some uncertainty was encountered in determining NMR shifts.

terized by the downfield shifts of the "interior" hydrogens (H_4 and H_5) and a sharpening of the NMR signals as deprotonation occurred.

With pyrazine **9** or its benzo derivatives **10** and **11** an unusual NMR spectra were obtained in which the interior protons moved


9   10   11
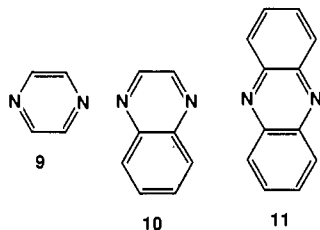
upfield by >0.5 ppm. The upfield shifts are nicely rationalized by the two-point binding of pyrazine postulated in eq 6. In the complex **12** the interior protons protrude into the strongly shielding regions of the aromatic system of the pyrazine nucleus.

$$2 + 9 \rightleftharpoons \qquad\qquad\qquad (6)$$
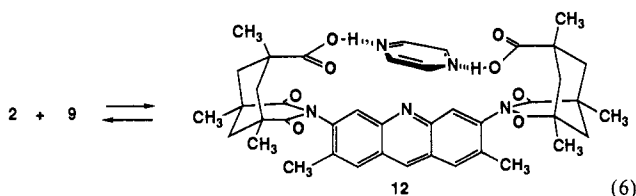
With **2** and DABCO the changes in NMR spectra were consistent with conventional deprotonation, but strong evidence was obtained for the formation of an unusually stable 1:1 complex. Specifically, a plot of the change in chemical shift of DABCO as a function of added **2** is graphed in the figure. This shows a fairly clean break at equimolar ratios. Treatment of such data by a variety of methods and the relative errors involved has been discussed by Deranleau.[8] For the DABCO the saturation curve is sufficiently complete that a Benesi–Hildebrand[9] double-reciprocal plot is expected to give reliable association constants. For pyrazine and weaker bases alternate treatments involving Scatchard[10] or Eadie[11] plots were used; these gave $K_{eq} = 1.4 \times 10^3$ for **9** (Table I).

(8) Deranleau, D. A. *J. Am. Chem. Soc.* **1969**, *91*, 4044–4050, 4050–4054.
(9) Benesi, H. A.; Hildebrand, J. H. *J. Am. Chem. Soc.* **1949**, *71*, 2703–2707.
(10) Scatchard, G. *Ann. N. Y. Acad. Sci.* **1949**, *51*, 660.
(11) Hofstee, B. H. J. *Nature (London)* **1959**, *184*, 1296. Eadie, G. S. *J. Biol. Chem.* **1942**, *146*, 85.

In an attempt to evaluate the extent to which reduced entropy contributes to the *chelation* of DABCO by the rigid **2**, as shown in **13**, a parallel complexation study using the nonmethylated **5**
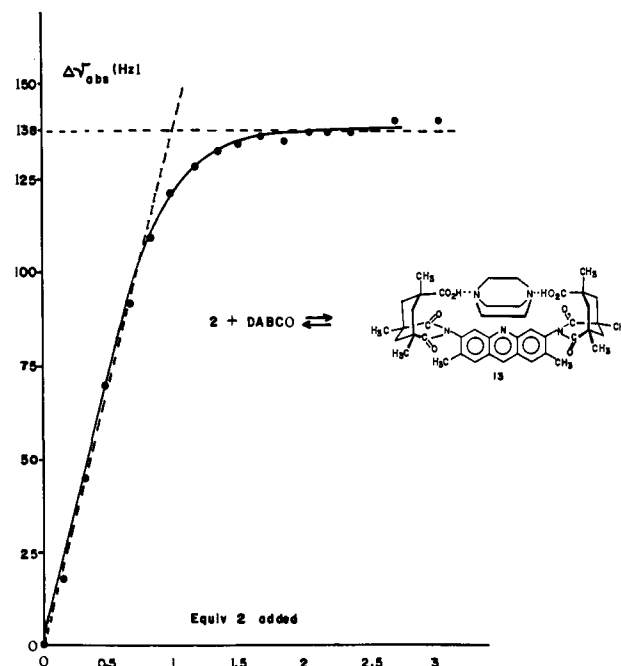
2 + DABCO ⇌

and DABCO was undertaken. This led to the value of $K_{eq} = 1.4 \times 10^4$ M⁻¹. The plots, however, showed more scatter than those involving **2**, and the break at 1:1 stoichiometry was a gradual one that suggested that stoichiometries other than 1:1 are possible. Even so, the evidence for two-point binding between **5** and DABCO could hardly be denied. This is presented below in the form of the NMR spectra of the aromatic regions of **5** in contact with Et_3N and DABCO. For Et_3N, rotation about the C_{aryl}–N_{imide} bonds leads to broadened signals for **14**, but the DABCO case
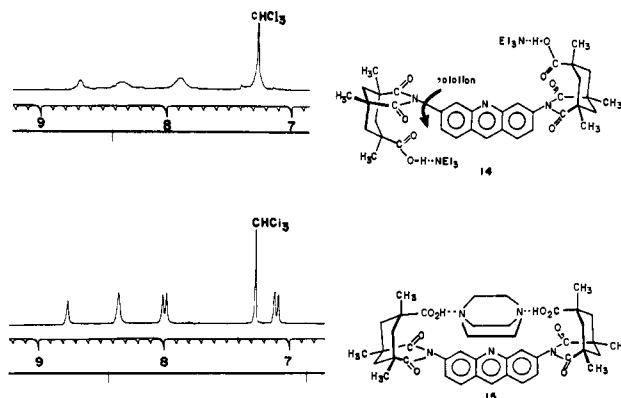
shows a sharp spectrum at ambient temperature. Such would be expected for either a single frozen, convergent conformation **15** or rapid exchange between all conformations. Since the spectra of **5** containing 1 equiv of DABCO were temperature independent, the former must be the case; DABCO's ability to bind two carboxyls stabilizes the converged diacid conformation. The difference in binding abilities of the rigid **2** and rotating **5** toward DABCO is worth some comment. The convergent conformation required for binding is one of four equally probable ground states. The 12-fold reduction in receptivity of **5** vs. **2** is beyond that figure expected on mere statistical grounds, but the scatter in the plots with **5** do not warrant detailed discussion.

For all bases studied, the rates of formation and dissociation of the complexes at room temperature were rapid on the NMR time scale. Only averaged spectra were observed; consequently, activation barriers must be low (<15 kcal/mol). A direct measure of this barrier was obtained for **2** and DABCO. When $^1/_2$ of an equivalent of base was added to **2** in CD_2Cl_2 and the temperature was *lowered* to 200 K, separate spectra for **2** and **13** were observed.

Convergent Functional Groups

J. Am. Chem. Soc., Vol. 109, No. 8, 1987 2429

The approximation formula led to a calculation of $\Delta G^{\ddagger}_c = 10.5$ kcal/mol at $T_c = 208$ K. This figure may be compared with dissociation barriers for crown ether complexes of primary ammonium ions (eq 7). These processes are generally believed to


$$(7)$$
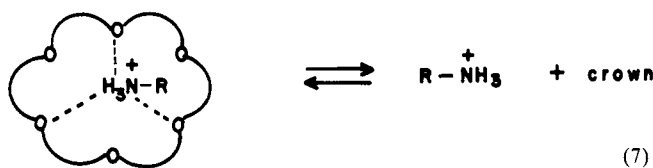
involve the breaking of three hydrogen bonds, and the dissociation barriers are in the 12–14 kcal/mol range.[12] For complex **13** then, charge–charge interactions contribute only a modest amount to stability; the viselike shape of **2** doesn't necessarily lead to a viselike grip!

A number of heterocyclic diamines of symmetrical structure were also examined, and the association constants are given in Table I. The use of symmetry was intended to simplify spectra and interpretation, and we were more or less successful in this strategy. Several trends emerge from the association constants of Table I.[13]

First, the binding energy associated with stacking interactions between aryl subunits in substrates and receptor was revealed by comparing pyrazine **9** with its benzo derivative, quinoxaline **10**. The 15-fold enhancement corresponds to about 1.5 kcal, and, given the nearly identical basicities of the two heterocycles, the enhancement is most likely due to stacking interactions as shown in **10a**. Indeed, upfield shifts of 0.1 and 0.25 ppm in $H_{5,8}$ and

10a
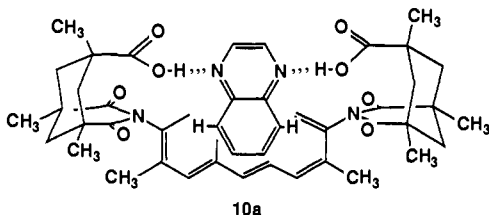
$H_{6,7}$, respectively, are best accommodated by this geometry. The reduction of binding to the more basic phenazine **11** is harder to rationalize but probably reflects some steric interactions between the carbonyl oxygen of the carboxyl and the peri hydrogens of the remote, unstacked ring as in **11a**. The upfield shifts observed with phenazine are about half of what is seen in quinoxaline; this value is consistent with a system showing rapid exchange between two equivalent stacking sites.

11a
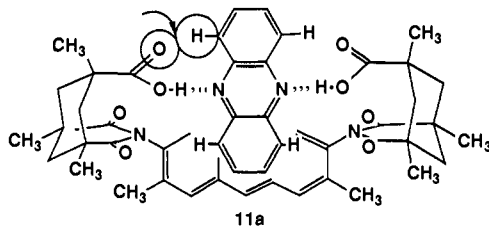
Second, the effects of geometry were observed by a study of pyrimidine **16**. Compared to pyrazine **9**, in which the N–N distance is about 2.8 Å, that distance in **16** is nearly 2.5 Å. The


16

effect of shape difference on the K_a was expected to provide a measure of the promiscuity of the diacids. The optimized distance between opposing oxygens in **2** is about 8 Å, but small angle

distortions in the imide function make large (± 1 Å) differences in this distance. In fact pyrimidine binds about half as well as pyrazine. The NMR spectra of the systems at 1:1 stoichiometry showed 0.15 ppm upfield shifts in the protons of pyrimidine but not in those of pyridazine. Thus stacking appears to be available for the base of inferior geometry, as suggested in **16a**.

16a
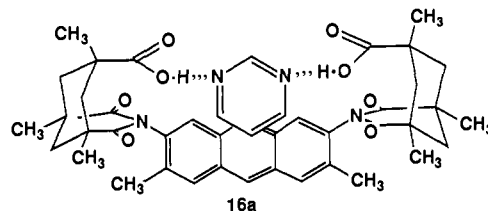
The basicities of the two heterocycles also differ. Unfortunately, too many differences exist between the two heterocycles; with the four variables—size, shape, stacking, and basicity—practically *any* result could be rationalized. The effects of increased surface contact are again seen in the enhanced binding of quinazoline **17**.

17
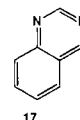
Third, another type of binding behavior was observed with imidazole **18**. Here a hydrogen bond donor and acceptor are in the same molecule, and complexation curves with **2** indicated a clean break at 2:1 (amine/acid) stoichiometry. Treatment of

18

the data in the form of a Hill plot showed a sigmoid curve characteristic[14] of interacting sites, with slope $n < 1$. This value corresponds to a *lowered*[15] affinity of the initial complex for a second imidazole, a situation that is probably caused by electrostatic forces. The binding of this relatively strong base probably involves some amount of proton transfer as suggested schematically in eq 8. This results in polarizing the carboxyls of **19a** in such

$$(8)$$
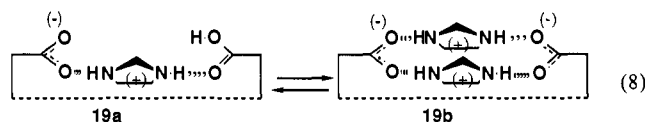
a manner that *both* become more receptive to hydrogen bonding—one as a proton donor and one as an acceptor. Subsequent introduction of a second imidazole as in **19b** forces propinquity of the two positive charges, and the overall effect is a lowering of K_2 relative to K_1.

A test of this interpretation would involve binding a similar substrate without creating as much charge. We had hoped that the weaker base benzimidazole **20** would serve this purpose, but

20
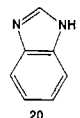
it proved even more difficult to add a second base to the 1:1 complex. Perhaps the stacking competition for the central acridine ring is the cause. We are currently exploring other substrates more likely to show positive cooperativity in binding to **2**.

Fourth, purine **21** was examined for its affinity for **2**. Here an intramolecular competition between imidazole and pyrimidine nuclei is available, and, apparently the imidazole wins. The upfield shifts in both the receptor and substrate are best accommodated by an equilibrium between stacking as in **22a** and the perpendicular
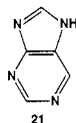
(12) Bradshaw, J. S.; Jones, B. A.; Davidson, R. B.; Christensen, J. J.; Lamb, J. D.; Izatt, R. M.; Morin, F. G.; Grant, D. M. *J. Org. Chem.* **1982**, *47*, 3362–3364.

(13) Preliminary communications: Rebek, J., Jr., Nemeth, D. *J. Am. Chem. Soc.* **1986**, *108*, 5637–5638.

(14) For an excellent discussion of this topic, see: Levitzki, A. *Mol. Biol., Biochem., Biophys.* **1978**, *28*, 15–27.

(15) Koshland, D. E., Jr. *Enzymes 3rd Ed.* **1970**, *1*, 341–396.

21

arrangement **22b** for the complexes of eq 9.

$$ \mathbf{22a} \rightleftharpoons \mathbf{2'} \rightleftharpoons \mathbf{22b} \tag{9} $$
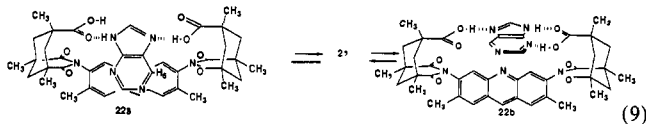
The freely rotating **5** was also tested with the less basic amines pyrazine **9** and quinoxaline **10**. Pyrazine showed reduced binding when compared to the fully locked counterparts **2**, and an average diminution of fivefold seems to be the cost of selecting the convergent conformation necessary for complexation. This figure is in good agreement with that obtained through the extraction of amino acids into $CDCl_3$ by **2** vs. **5**, where it was observed[2c] that **5** was only about one-fifth as effective as **2**.

Rather surprisingly, the base quinoxaline binds *better* to **5** (K = 2.9 × 10^4) than to **2** (K = 2.3 × 10^4), a result that was confirmed by direct competition experiments involving the two diacids. One explanation is offered in **23**; maximal overlap[16] of the aryl groups requires some rotation about the C_{aryl}–N bond. The ortho methyl group of **10a** resists this motion more than the smaller H of **5**.

23
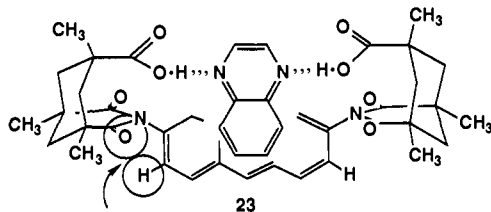
Finally, pyridine was tested with **2**. This base also showed upfield shifts for the protons lining the molecular cleft, but the binding curves showed a gradual break at 1:1 stoichiometry. The association of a second pyridine is quite difficult, and the figure quoted in Table I for this process has a large uncertainty. Even so, this case demonstrates the advantages of a weak base with proper shape (pyrazine) vs. the stronger base (pyridine). In direct competitions, pyrazine is complexed even when excess pyridine is present; only with pyrazine is the receptor able to act in its capacity as a molecular chelate which converges on the substrate from opposite sides.

Conclusions and Perspectives

The recognition of molecules having appropriate size, shape, and complementary functionality has been demonstrated. The use of a molecular cleft[17] offers the advantage of efficient assembly, and the unique feature of convergent functional groups introduces, at least to model systems, a high degree of directionality[18] in substrate/receptor interactions. In large part the directionality is due to the nature of the binding forces involved, and these provide a complement to those offered by other systems.[19]

It will be interesting to see if these molecular clefts can be derivatized with functional groups which can converge on and recognize guest species of any specified structure or chemistry, since other model receptors tend to be quite specialized. For

(16) For a discussion of alternative geometries for aryl–aryl interactions, see: Burley, S. K.; Petsko, G. A. *Science (Washington, DC)* **1985**, *229*, 23–28.

(17) For another host system with this shape, see: Cornforth, J.; Ridley, D.; Sierakowski, A. F.; Uguen, D.; Wallace, T. W. *J. Chem. Soc., Perkin Trans. 1* **1982**, 2333–2339.

(18) Rebek, J., Jr.; Duff, R. J.; Gordon, W. E.; Parris, K. *J. Am. Chem. Soc.* **1986**, *108*, 6068–6069.

(19) For an overview, see: Vogtle, F.; Muller, W. M. *J. Inclus. Phen.* **1984**, 369–386. An impressive array of complexes involving *crystal lattice* clefts are available: Weber, E.; Csoregh, I.; Stensland, B.; Czugler, M. *J. Am. Chem. Soc.* **1984**, *106*, 3297–3306. Weber, E.; Josel, H.-P.; Puff, H.; Franken, S. *J. Org. Chem.* **1985**, *50*, 3125–3132.

example, the recognition of charged species has been well-developed; the classic chelation chemistry of metal ions has now been refined to an extraordinary degree by macrocyclic polyethers toward spherical ions such as Li$^+$.[20] For larger ions, most of the attention in polyethers has been directed toward the primary ammonium function. Consequently, recognition at the molecular level has almost exclusively involved ammonium "knobs"[21] rather than other sites on a substrate molecule. It is therefore a good omen that both stacking and charged interactions have recently been observed in the binding of **1** to zwitterionic forms of aromatic amino acids. We shall report on these developments in the sequel.

Experimental Section

I. Synthesis. *cis,cis*-**Trimethyl 1,3,5-Trimethylcyclohexane-1,3,5-tricarboxylate (7).** Literature methods were used to hydrogenate trimesic acid;[5a] esterification with $SOCl_2/MeOH$ and distillation gave material[5b] suitable for use in the alkylation.

All operations were carried out in flame dried glassware under a dry nitrogen atmosphere. Lithium diisopropyl amide (LDA) was generated at 0 °C by the addition of 146 mL of *n*-butyllithium (3.3 equiv) to 17.9 mL of diisopropylamine (3.3 equiv) in 100 mL of dry Et_2O. After having been stirred for 30 min, 10 g of triester **6** in 100 mL of Et_2O was added dropwise. The mixture was stirred at 0 °C for 2 h, then 20 mL of dimethyl sulfate was added, and stirring was continued overnight at room temperature. The resulting solution was filtered, washed successively with H_2O, 1 N HCl, and brine, and then dried over $MgSO_4$. Solvent removal gave 10.8 g of a yellow oil. GC analysis indicated a 85:15 mixture of the cis,cis and cis,trans isomers with an overall purity of 96%. Crystallization from pentane/Et_2O afforded the cis,cis isomer as colorless prisms, 7.2 g (62%), mp 80–81 °C (lit. 79–81 °C):[3] ^{1}H NMR ($CDCl_3$) δ 0.95 (d, J = 13 Hz, 3 H), 1.20 (s, 9 H), 2.71 (d, J = 14 Hz, 3 H), 3.60 (s, 9 H).

Alternatively, separation of the alkylation mixture can be accomplished by preparative HPLC on a Waters Prep-500 system by using silica columns and 10% EtOAc/hexane as eluent.

1,3,5-Trimethylcyclohexane-1,3,5-tricarboxylic Acid (3). The triester **7** (5 g) was dissolved in a mixture of 50 mL of CH_3OH and 50 mL of 3 N NaOH. The solution was heated to 65 °C and stirred for 12 h. The CH_3OH was removed at reduced pressure, and the aqueous solution was cooled and adjusted to pH 1 with concentrated HCl. The triacid **3** appeared as a white precipitate, 4.1 g (95%), mp 240–247 °C (lit. 230–245 °C):[3] NMR (pyridine-d_5) δ 1.56 (s, 9 H), 1.53 (d, J = 14 Hz, 3 H), 3.3 (d, J = 13.5 Hz, 3 H).

Preparation of the Receptors. The synthesis of the diacid **2** and its dimethyl ester **2a** has already been described.[1a] Similar procedures were used to prepare **4** and **5**. A mixture of 254 mg of 2,7-diaminofluorene (Aldrich) and 766 mg of the triacid **3** were ground together and then heated in a loosely stoppered flask for 5 h in a sand bath at ~240 °C. The mixture fused but did not liquefy. The cooled reaction mixture was dissolved in 100 mL of CH_2Cl_2, filtered through Celite, and then evaporated to give 976 mg of a brown solid. Trituration with 50 mL of ether overnight dissolved ca. 300 mg of the anhydride of **3**. The ether insoluble portion was dissolved in CH_2Cl_2 (100 mL) and washed with 30 mL of 1 N HCl and then saturated brine solution. Drying (Na_2SO_4) and then evaporation gave 615 mg (75%) of **4**, mp > 275 °C: ^{1}H NMR (300 MHz, $CDCl_3$) 296 K δ ca. 7.27 (br, 4 H), 6.80 (br, 2 H), 3.15 (br, 2 H), 2.89 (d, J = 14 Hz, 4 H), 2.17 (d, J = 14 Hz, 2 H), 1.50 (d, J = 14 Hz, 2 H), 1.37 (s, 12 H, s, 6 H, d, 4 H), 2.29 (d, J = 13 Hz, 2 H), 1.63 (d, J = 13 Hz, 2 H), 1.43 (d, J = 14 Hz, 4 H), 1.34 (s, 22 H); IR (cast film on NaCl) ν (cm^{-1}) 2968.8, 2932.2, 1730, 1720, 1705, 1684.1, 1464.2, 1182.5, 731.1; ^{13}C NMR (75.469 MHz, 5% Me$_2$SO-d_6 in $CDCl_3$) δ 177.5 (s, carboxyl, C=O), 176.5 (s, imide, C=O), 143.7 (s, aryl C), 140.4 (s, aryl C), 134.4 (d, J = 8 Hz, aryl C), 127.0 (d, J = 162 Hz, aryl C–H), 124.9 (d, J = 160 Hz, aryl C–H), 119.6 (d, J = 161 Hz, aryl C–H), 43.9 (t, J = 132 Hz, cyclohexyl CH), 41.3 (s, cyclohexyl C), 40.45 (s, cyclohexyl C), 36.6 (t, J = 133 Hz, benzyl CH$_2$), 30.7 (q, J = 130 Hz, CH$_3$), 25.7 (q, J = 128 Hz, CH$_3$).

The dimethyl ester **4a** was prepared with CH_2N_2 and then purified by preparative TLC (R_f 0.275, 1:1 EtOAc/hexane, 2 mm silica gel), mp 231–232 °C: ^{1}H NMR (300 MHz, $CDCl_3$, 296 K) δ 7.77 (d, J = 8.1 Hz, 2 H), 7.29 (br, 2 H), 7.15 (br, 2 H), 3.90 (s, 2 H), 3.62 (s, 6 H), 2.88 (d, J = 14 Hz, 4 H), 2.16 (d, J = 13 Hz, 2 H), 1.49 (d, J = 13 Hz,

(20) Cram, D. J.; Kaneda, K.; Helgeson, R.; Brown, S. B.; Knobler, C. B.; Maverick, E.; Trueblood, K. N. *J. Am. Chem. Soc.* **1985**, *107*, 3645–3657, and references therein.

(21) Lehn, J.-M. *Science (Washington, DC)* **1985**, *227*, 849–856. For selective binding of uncharged species to crown ethers, see: Rebek, J., Jr.; Marshall, L. *J. Am. Chem. Soc.* **1983**, *105*, 6668–6670.

2 H), 1.36 (s, 12 H), 1.29 (s, 6 H, d, 4 H); IR (cast film on NaCl) ν (cm^{-1}) 2966.9, 2930.2, 1730, 1684.1, 1458, 1178, 731; calcd for C$_{39}$-H$_{44}$N$_2$O$_8$ 668.3098, found 668.3082 (M$^+$).

The diacid chloride of **4** was prepared in 80% yield with SOCl$_2$ (neat) and purified by chromatography on silica gel by using EtOAc as eluent, mp > 270 °C: ^{1}H NMR (300 MHz, CDCl$_3$) δ 7.82 (d, J = 8.10 Hz, 2 H), 7.25 (br, 2 H), 7.10 (br, 2 H), 3.94 (s, 2 H), 2.95 (d, J = 14.5 Hz, 4 H), 2.21 (d, J = 13.3 Hz, 2 H), 1.54 (d, J = 13.4 Hz, 2 H), 1.45 (s, 6 H), 1.39 (s, 12 H, d, 4 H); ^{13}C NMR (75.469 MHz, CDCl$_3$) δ 180.1 (s, C=O), 175.8 (s, C=O), 144.4 (s, aryl C), 141.3 (s, aryl C), 134.2 (s, aryl C), 126.6 (d, J = 144 Hz, aryl C–H), 124.6 (d, J = 158 Hz, aryl C–H), 120.6 (d, J = 160 Hz, aryl C–H), 44.8 (t, J = 128 Hz, cyclohexyl CH$_2$), 44.0 (t, J = 120 Hz, cyclohexyl, CH$_2$), 40.7 (s, cyclohexyl C), 37.1 (t, J = 137 Hz, benzyl CH$_2$), 30.4 (q, J = 132, CH$_3$), 25.9 (q, J = 127, CH$_3$); IR (cast film on NaCl) ν (cm^{-1}) 2968.8, 2932.2, 1790, 1732.3, 1714.9, 1693.7, 1682.1, 1462.2, 1180.6, 731.1.

An 89-mg sample of the diacid chloride was partly dissolved in 50 mL of *p*-dioxane. Ammonia was bubbled into the mixture for 3 h. The mixture was then evaporated, and the residue was dissolved in 150 mL of CH$_2$Cl$_2$, washed with 50 mL of saturated NaHCO$_3$ and then brine, and dried over Na$_2$SO$_4$. The CH$_2$Cl$_2$ was evaporated to give 90 mg of the diamide **4b**, mp > 275 °C: ^{1}H NMR (300 MHz, acetone-d_6) δ 7.75 (d, aryl, 2 H), ~7 (br, aryl C–H, 4 H), 6.76 (s, 2 H, amide NH), 6.40 (s, 2 H, amide NH), 3.83 (s, 2 H), 2.76 (d, 4 H, also H$_2$O), 2.23 (d, 2 H), 1.57 (d, 2 H), 1.37 (d, 4 H), 1.35 (s, 18 H); ^{13}C NMR (75.469 MHz, Me$_2$SO-d_6) δ 177.0 (s, amide C=O), 176.3 (s, imide C=O), 143.2 (s, aryl C), 139.9 (s, aryl C), 135.7 (s, aryl C), 127.5 (d, J = 145 Hz, aryl C–H), 125.6 (d, J = 163 Hz, aryl C–H), 119.6 (d, J = 168 Hz, aryl C–H), 43.4 (t, J = 128 Hz, cyclohexyl CH$_2$), 42.78 (s, cyclohexyl C), 41.2 (s, cyclohexyl C), 36.4 (t, J = 135 Hz, benzyl CH$_2$), 25.8 (q, J = 128 Hz, CH$_3$), 25.6 (q, J = 127 Hz, CH$_3$; IR (cast film on NaCl) ν (cm^{-1}) 2965, 2928, 1732, 1684, 1653, 1464, 1358, 1184, 731.
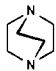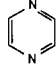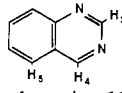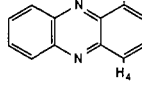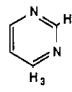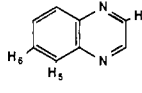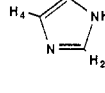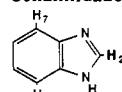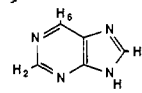
The corresponding derivative of **5** was prepared in similar manner. For **5** itself, mp > 275 °C: ^{1}H NMR (300 MHz, CD$_3$OD) δ 9.14 (s, 1 H), 8.18 (d, J = 9.5 Hz, 2 H), 8.04 (br, 2 H), 7.50 (br, 2 H), 2.83 (d, J = 14 Hz, 4 H), 2.38 (d, J = 14 Hz, 2 H), 1.67 (d, J = 14 Hz, 2 H), 1.48 (d, J = 14 Hz, 4 H), 1.39 (s, 18 H); ^{13}C NMR (75.469 MHz, Me$_2$SO-d_6) δ 177.7 (s, carboxyl C=O) 176.2 (s, imide C=O), 148.4 (s, aryl C), 138.6 (s, aryl C), 135.8 (d, J = 169 Hz, aryl C–H), 128.2 (d, J = 165 Hz, aryl C–H), 127.5 (d, J = 156 Hz, aryl C–H), 125.5 (s, aryl C), 121.2 (d, J = 160 Hz, aryl C–H), 43.2 (t, J = 136 Hz, cyclohexyl CH$_2$), 42.0 (t, J = 131 Hz, cyclohexyl CH$_2$), 41.2 (s, cyclohexyl C), 40.21 (s, cyclohexyl C), 30.65 (q, J = 128 Hz, CH$_3$), 25.52 (q, J = 128 Hz, CH$_3$); IR (cast film on NaCl) ν (cm^{-1}) 2970.7, 2934.1, 1734.2, 1716.9, 1686.0, 1458.4, 1180.6.

The dimethyl ester **5a** was prepared with diazomethane and then purified by preparative TLC (R_f 0.125, 1:1 EtOAc/hexane, 2 mm silica gel) to a light tan solid, mp 195–197 °C: ^{1}H NMR (300 MHz, CDCl$_3$, 296 K) δ 8.76 (s, 1 H), 8.00 (d, J = 8.8 Hz, 2 H + 2 H), 7.38 (br d, 2 H), 3.64 (s, 6 H), 2.91 (d, J = 14 Hz, 4 H), 2.22 (d, J = 13 Hz, 2 H), 1.53 (d, J = 13 Hz, 2 H), 1.38 (s, 12 H), 1.31 (s, 6 H, d, 4 H); IR (cast film on NaCl) ν (cm^{-1}) 2966.9, 2934.1, 1732.3, 1684.1, 1456.4, 1176.7; calcd for C$_{39}$H$_{43}$N$_3$O$_8$ 681.3050, found 681.3039 (M$^+$).

Derivatives of the Acridine 2. A solution of 0.9 g of the diacid **2** in 300 mL of CH$_2$Cl$_2$ (distilled from CaH$_2$) was placed in a 500-mL, three-necked flask equipped with a CaCl$_2$ drying tube. Diisopropyl-ethylamine (1.9 mL, 6 equiv) and DMF (20 μL) were added, and the solution was cooled to 0 °C. Thionyl chloride (0.58 mL, 4 equiv) was added, and the solution was stirred for 1 h, then warmed to 25 °C, and washed with H$_2$O (50 mL), 10% citric acid (50 mL), and saturated NaHCO$_3$ (50 mL). The organic layer was dried over MgSO$_4$, concentrated to 50 mL, and then diluted with 200 mL of hexane giving the diacid chloride as a yellow precipitate, 760 mg (74%), mp > 340 °C: ^{1}H NMR (CDCl$_3$) δ 1.40 (d, J = 13 Hz, 4 H), 1.42 (s, 12 H), 1.52 (s, 6 H), 1.61 (d, J = 13 Hz, 4 H), 2.18 (s, 6 H), 2.25 (d, J = 13.3 Hz, 2 H), 3.00 (d, J = 13 Hz, 4 H), 7.80 (s, 2 H), 8.13 (s, 2 H), 8.55 (s, 1 H); IR (KBr pellet) ν (cm^{-1}) 2972, 2932, 1805, 1736, 1691, 1647, 1460, 1383, 1236.

Acridine Diamide 2b. Anhydrous ammonia gas was bubbled through a solution of the diacid chloride above (50 mg) in 10 mL of dry THF. After 20 min the turbid solution was evaporated, and the residue was taken up in CH$_2$Cl$_2$, washed with H$_2$O (2 × 20 mL), dried, and evaporated giving the diamide **2b** in quantitative yield, mp > 340 °C: ^{1}H NMR (CDCl$_3$) δ 1.2 (s, 6 H), 1.3 (s, 12 H), 1.28 (d, J = 13 Hz, 4 H), 1.5 (d, J = 13 Hz, 2 H), 2.1 (d, J = 13 Hz, 2 H), 2.2 (s, 6 H), 2.73 (d, J = 13.3 Hz, 2 H), 6.2 (s, 2 H NH), 7.42 (s, 2 H, NH), 7.8 (s, 2 H), 8.3 (s, 2 H), 8.6 (s, 1 H); IR ν (cm^{-1}) 3505, 3378, 2965, 2930, 1730, 1686, 1599, 1462, 1188 (All measurable amounts of water could be removed from **2b** by vacuum drying at 80 °C for 12 h).

Table II. Complexes of **2** with Heterocyclic Amines

substrate amine	receptor/ substrate ratio	chem shift of receptor (ppm) + = downfield	chem shift of substrate (ppm) + = downfield
DABCO	1:1	(a) 8.27 (+0.12) (b) 7.79 (0) (c) 8.56 (−0.06) (a) = H$_4$, H$_5$; (b) = H$_1$, H$_8$; (c) = H$_9$	3.24 (+0.44)
pyrazine **9**	4:1	(a) 7.69 (−0.45) (b) 7.60 (−0.2) (c) 8.41 (−0.2)	8.70 (+0.05)
	1:2	(a) 8.08 (−0.05) (b) 7.79 (0) (c) 8.62 (0)	
quinoxaline **10**	1:1	(a) 7.70 (−0.45) (b) 7.30 (20.2) (c) 8.29 (−0.3)	(2,3) 9.37 (+0.5) (5,8) 7.86 (−0.3) (6,7) 7.43 (−0.4)
phenazine **11**	1:1	(a) 7.95 (−0.2) (b) 7.69 (−0.1) (c) 8.52 (−0.1)	(1) 8.27 (0) (2) 7.681 (−0.2)
	3:1	(a) 7.63 (−0.5) (b) 7.63 (−0.15) (c) uncertain	(1) 8.27 (0) (2) 7.86 (0)
pyrimidine **16**	1:1	(a) 7.95 (−0.2) (b) 7.73 (−0.05) (c) 8.50 (−0.1)	(2) 9.45 (+0.15) (4,6) 8.75 (−0.05) (5) 7.18 (−0.15)
	2:1	(a) 7.90 (−0.25) (b) 7.73 (−0.05) (c) 8.50 (−0.1)	(2) 9.40 (+0.1) (4,6) 8.75 (−0.05) (5) 7.23 (−0.1)
quinazoline **17b**	1:1	(a) 8.04 (−0.1) (b) 7.64 (−0.15) (c) 8.37 (−0.3)	(2) 9.45 (−0.02) (4) 9.35 (−0.01) (5) 7.75 (−0.20) (6) 7.55 (−0.15) (7) 7.80 (−0.15) (8) 7.95 (−0.13)
imidazole **19**	1:1.5	(a) 8.21 (+0.005) (b) 7.73 (−0.05) (c) 8.48 (−0.15)	(2) 8.92 (+1.2) (4,5) 6.65 (−0.5)
	1:1	(a) 8.06 (−0.05) (b) 7.68 (−0.1) (c) 8.43 (−0.2)	(2) 8.68 (+1.0) (4,5) 6.65 (−0.5)
benzimidazole **21**	1:1	(a) 8.19 (+0.05) (b) 7.65 (−0.15) (c) 8.32 (−0.3)	(2) 8.47 (+0.4) (4,7) 7.27 (−0.41) (5,6) 6.79 (−0.52)
purine **22**	1:2	(a) 7.74 (−0.4) (b) 7.65 (−0.15) (c) 8.34 (−0.3)	(2) 9.08 (−0.15) (8) 8.28 (+0.03) (6) 8.82 (−0.25)
	1:1	(a) 7.72 (−0.4) (b) 7.64 (−0.15) (c) 8.32 (−0.3)	(2) 9.11 (−0.1) (8) 8.26 (+0.01) (6) 8.86 (−0.2)

II. Association Constants. Binding of 2 to DABCO. A 100-μL sample of 4.5 × 10^{-3} M DABCO in CDCl$_3$ was diluted with 300 μL of CDCl$_3$ in a 5 mm × 8 in. NMR tube. A starting spectrum was taken. Aliquots of 7.6 × 10^{-4} M **2** in CDCl$_3$, usually 100 μL, were added, and a spectrum was recorded after each addition. The downfield movement of the DABCO singlet as the amount of **2** in the tube increased was measured as $\Delta\nu_{obsd}$ relative to the starting chemical shift ν_0.

$$\Delta\nu_{obsd} = \nu - \nu_0$$

A plot of $\Delta\nu_{obsd}$ vs. equiv of **2** is shown in the figure with structure **13**. NMR studies of the other amines of Table I were performed in a similar manner. Association constants were obtained from least-squares slopes of Benesi-Hildebrand[9] or Eadie-Hofstee[11] plots, depending on the degree of saturation that could be reached in the titration protocol. These results are given in Table II.